

Decision-making and control with metasurface-based diffractive neural networks

Jumin Qiu¹, Tianbao Yu^{1*}, Lujun Huang^{2*}, Andrey Miroshnichenko³ and Shuyuan Xiao^{4,5*}

¹School of Physics and Materials Science, Nanchang University, Nanchang, 330031, Jiangxi, China.

²School of Physics and Electronic Science, East China Normal University, Shanghai, 200241, China.

³School of Engineering and Information Technology, University of New South Wales Canberra, Canberra, ACT 2600, Australia.

⁴Institute for Advanced Study, Nanchang University, Nanchang, 330031, Jiangxi, China.

⁵Jiangxi Key Laboratory for Microscale Interdisciplinary Study, Nanchang University, Nanchang, 330031, Jiangxi, China.

*Corresponding author(s). E-mail(s): yutianbao@ncu.edu.cn; ljuhuang@mail.sitp.ac.cn; syxiao@ncu.edu.cn;

Contributing authors: qijumin@email.ncu.edu.cn; andrey.miroshnichenko@unsw.edu.au;

Abstract

The ultimate goal of artificial intelligence is to mimic the human brain to perform decision-making and control directly from high-dimensional sensory input. All-optical diffractive neural networks provide a promising solution for implementing artificial intelligence with high-speed and low-power consumption. To date, most of the reported diffractive neural networks focus on single or multiple tasks that do not involve interaction with the environment, such as object recognition and image classification. In contrast, the networks that can perform decision-making and control, to our knowledge, have not been developed yet. Here, we propose using deep reinforcement learning to implement diffractive neural networks that imitate human-level decision-making and control capability. Such networks allow for finding optimal control policies through interaction with the environment and can be readily realized with the dielectric metasurfaces. The superior performances of these networks are verified by engaging three types of classic games, Tic-Tac-Toe, Super Mario Bros., and Car Racing, and achieving the same or even higher levels comparable to human players. Our work represents a solid step of advancement in diffractive neural networks, which promises a fundamental shift from the target-driven control of a pre-designed state for simple recognition or classification tasks to the high-level sensory capability of artificial intelligence. It may find exciting applications in autonomous driving, intelligent robots, and intelligent manufacturing.

1 Introduction

Artificial intelligence (AI) is to imitate the functions of neurons in performing decision-making by creating hierarchical artificial neural networks. It has found many exciting applications in computer vision[1, 2], natural language processing[3, 4], and data mining[5]. Except for electronics and computer science applications, artificial neural networks have been applied to optimize the design of photonic devices, including metamaterials and metasurface, significantly facilitating the performance of photonic devices beyond the conventional inverse design strategy [6–18]. Recently, optical neural networks have drawn tremendous attention because it provides a compelling route of processing information at the speed of light but with low energy consumption and massive parallelism compared to the electronic-circuit-based neural network[19–24]. In the pioneering work by Lin et al.[25], a diffractive neural network comprising multiple layers of three-dimensional printed diffractive optical elements operating at terahertz was first proposed for inference and prediction through parallel calculations and dense interconnection at the speed of light. Such architecture has been effectively validated in performing specific inference functions, such as image classification[26–31], object detection[32, 33], and logic operation[34]. Driven by the pursuit of a compact on-chip system, optical metasurfaces made of an array of subwavelength meta-atoms are introduced to replace the bulky diffractive optical elements for high-density integration. Metasurfaces provide the unprecedented ability to manipulate the wavefront of light. They thus are widely used to implement multi-sophisticated functions, such as holography and computational imaging [35–43]. More recently, a multi-channel classifier framework of on-chip diffractive neural networks, which can perform multiple tasks in the visible wavelength region, has been theoretically proposed and experimentally demonstrated by leveraging the polarization-multiplexed metasurface [44]. Although optical diffractive neural networks have witnessed significant progress in the past few years, their functions mainly focus on image classification and object recognition and do not involve any interaction with the environment. To our knowledge, human-level AI based on diffractive neural networks that can perform

decision-making and control has not yet been developed.

In this work, we bring the capability of decision-making and control directly from high-dimensional sensory inputs to diffractive neural networks. The networks build upon deep reinforcement learning to interact with a simulated environment for optimal control policies. The training process of policy is based solely on deep reinforcement learning from self-play without dataset or guidance. Each layer of the diffractive networks is featured by a phase profile mapping and thus can be immediately realized by the dielectric metasurface. The effectiveness of the proposed diffractive neural networks is validated with three typical games, Tic-Tac-Toe, Super Mario Bros., and Car Racing. This work enables a fundamental shift from the target-driven control of a pre-designed state for simple recognition or classification tasks to the human-imitative AI, revealing the potential of optoelectronic and all-optical on-chip integrated AI systems to solve complex real-world problems. We envision that such diffractive neural networks may find promising applications in autonomous driving, industrial robots, and intelligent manufacturing, aiming to enhance human life in every aspect.

2 Results

2.1 The network for decision-making and control

The working principle of the diffractive neural network for decision-making and control is illustrated in Fig. 1a–c, using an example of playing Nintendo’s classic video game Super Mario Bros. In general, a human player goes through seeing, understanding, and making a decision in each step, and these perception and control behaviors loop until the game is over. In order to play games in a human-like manner, the network necessitates the sensory capability to capture continuous, high-dimensional state spaces and the controllable execution ability of sequences of different behaviors. The diffractive neural network shown in Fig. 1b comprises the specific free-space configuration: an input layer with images encoded using an optical modulation device, hidden layers made of diffractive metasurfaces with meta-neurons encoding phases of transmitted waves, and an output layer

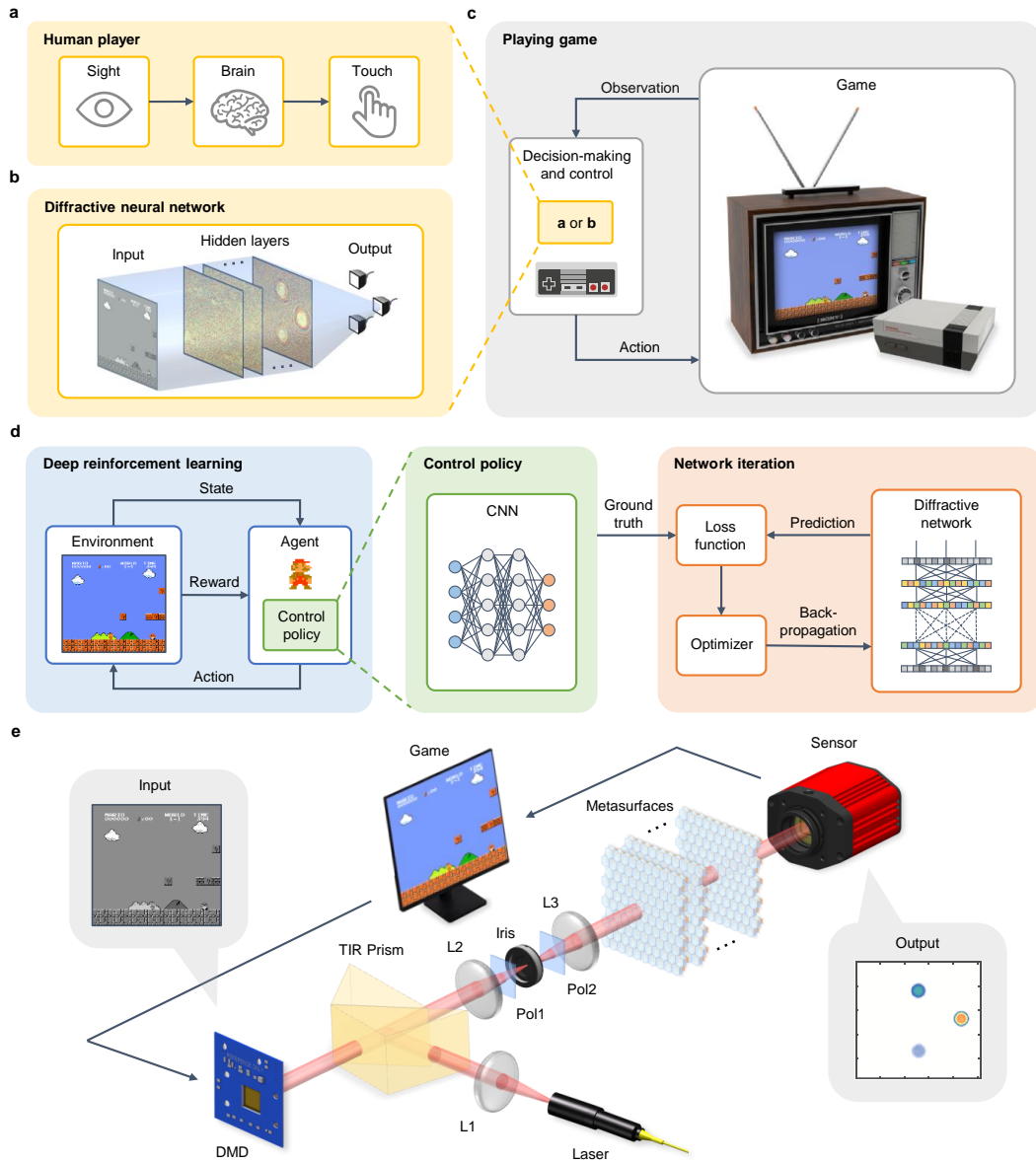


Fig. 1 The diffractive neural network for decision-making and control. **a–c** The proposed network plays the video game of Super Mario Bros. in a human-like manner. In the network architecture, an input layer captures continuous, high-dimensional game snaps (seeing), a series of metasurface diffractive layers choose a particular action through a learned control policy for each situation faced (making a decision), and an output layer maps the intensity distribution into preset action regions to generate the control signals in the games (controlling). **d** Training framework of policy and network. Deep reinforcement learning through an agent interacts with a simulated environment to find a near-optimal control policy represented by a CNN, which is employed as the ground truth to update the diffractive neural network by error back-propagate algorithm. **e** The experimental setup of the metasurface-based diffractive neural network.

in which the computational results are imaged into. Different from common neural networks in which the computations engage mostly linear transformations, such as convolution, the propagation and diffraction of light provide nonlinearity

to diffractive neural networks. This means that diffractive neural networks exhibit nonlinear mapping ability even without activation functions.

More importantly, the proposed framework for decision-making and control combines deep reinforcement learning and diffractive neural network into a training procedure, allowing interaction between the game and the agent to learn control policies that can be implemented through the optical computing platform. The method observes each state within the game environment and chooses a particular action through a learned control policy for each situation faced. Then the changed environment generates observation of the new state and makes the next action, and continuously updates the control policy in the loop. Unlike the previous optical networks, the input images from each video game frame are continuous high-dimensional sensory data. Furthermore, the execution procedure, such as playing games, is essentially a type of interactive control rather than the one-way recognition for single objectives such as written digits or fashion items.

To address the complexity of imitating human players on the optical platform, we develop the training framework of policy and network shown in Fig. 1d, using a combination of novel and existing general-purpose techniques for neural network architectures. As shown in the middle block of Fig. 1d, central to the architecture is a control policy $\pi_{\theta}(a|s)$, which is represented by a convolutional neural network (CNN) with parameters θ that makes observations s as inputs and takes actions a as outputs by optimizing the reward of games of self-play. Note that the training epoch of deep reinforcement learning is markedly more than that of the diffractive neural networks due to the training of policies starting from completely random behavior. Thus, we developed the training process approach with two main phases to eliminate unnecessary computations. Firstly, deep reinforcement learning through an agent interacts with a simulated game environment to find a near-optimal control policy to meet the specified goals. Secondly, the control policy is employed to update the diffractive neural network by error back-propagation algorithm.

In the first phase, a deep reinforcement learning algorithm collects data to find a control policy with respect to the specific reward function through interaction with the game environment. The algorithm utilizes an agent to play the game in a specific environment with a well-designed reward function to attain the desired outcome.

The states of these games need to satisfy the Markov property that the information of a certain state contains all relevant histories. Thus it is possible to perform actions in the current state and move to the next state without considering the previous states. The agent interacts with the environment through a sequence of observations, actions, and rewards. At each step of interaction, the agent observes the state of the environment to decide on an action to take and then gives rewards based on the game result. Based on the reward, the neural network decides the best action for each step and continuously updates the policy using proximal policy optimization (PPO)[45] to find the most appropriate action. After testing, the trained policies can all complete the respective game. Compared with the previous studies, the algorithm only requires game rules without the need for human data, guidance, or domain knowledge, avoiding the dependence of the performance on the dataset's quality.

In the second phase, the control policy is transferred onto the diffractive neural network. During the learning procedure, the optimal control policy modeled using the CNN is utilized as the ground truth. Meanwhile, following the forward propagation model based on Huygens' principle and Rayleigh-Sommerfeld diffraction, the encoded input light can be directed into any desired location at the output layer via the learnable transmission coefficients, that is, phase profiles of metasurfaces in the network. The energy distributions clustered in the target detection region imply the prediction results. The transmission coefficients at each diffractive metasurface layer should be adequately trained via the error back-propagation algorithm and a loss function with mean square error (MSE), which is defined to evaluate the performance between the output intensities and the ground truth target. The adaptive moment estimation (Adam)[46], an algorithm for first-order gradient-based optimization of stochastic objective functions, is adopted to reduce the loss function. Then the gradient of the loss function with respect to all the trainable network variables is backpropagated to iteratively update the network during each cycle of the training phase until the network converges.

Once the training is completed, the target phase profiles of the metasurface diffractive layers

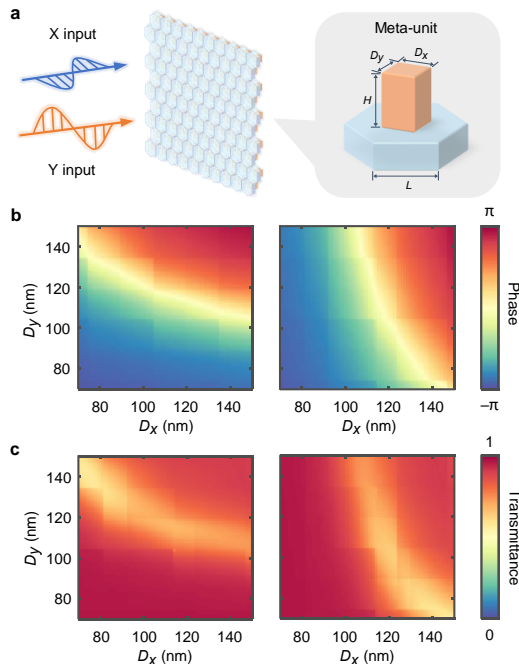


Fig. 2 The complex-valued transmission coefficient of the metasurface. **a** The unit cell. The phase **b** and transmittance **c** of honeycomb metasurface under x- and y-polarized light at 633 nm. Since the nanopillars are rectangular, the effective refractive indices along the two crossed axes are different, thus achieving polarization multiplexing.

are determined, which are ready to connect physical and digital worlds for optical neuromorphic computing. Here we choose carefully arranged silicon nanopillars on a quartz substrate as building blocks due to the mature silicon-on-insulator (SOI) fabrication technology. For the sake of simplicity, the operating wavelength is set as 633 nm. Note the higher integration and transmittance than the common square lattice. The honeycomb lattice is adopted here to enable more stable responses and higher accuracy; see Methods and Supplementary Fig. 2 for a detailed design principle of the metasurface. By adjusting the length and width of these nanopillars, we can modify the transmitted phase of meta-atoms covering almost 2π and then construct the specific metasurfaces according to the relations between phase profiles and geometry parameters. In particular, the two-fold symmetry of the nanopillars introduces the birefringence and distinct phase responses for incident light with orthogonal polarization

states, making it possible to achieve polarization-multiplexed networks under x- and y-polarization incidence. Fig. 2 shows the phase and transmittance vs. geometry parameters under x- and y-polarization light.

Thanks to the rapid development of nanofabrication, the multi-layer diffractive metasurfaces can be readily fabricated by standard procedures, including electron beam lithography and reactive ion etching, which have been widely used in both plasmonic and dielectric meta-optics[44, 47, 48]. They can also be obtained with the recently emerging two-photon nanolithography method[49, 50]. Moreover, the operating mechanism and design principle of the proposed diffractive networks are universal and thus can be generalized to other operating wavelengths like terahertz and microwave (despite lower neuron density) in which the fabrication techniques are more easily accessible[28, 30, 51]. The experimental setup of the metasurface-based diffractive neural network is shown in Fig. 1e. A laser at a working wavelength of 633 nm is collimated using a lens (L1) and is reflected onto the suitable incident angle for a digital micromirror device (DMD) by a total internal reflection prism (TIR prism). The input image data are optically encoded and modulated by DMD, followed by two relay lenses (L2 and L3), while the linear polarizers can be embedded to adjust the incident light polarization. The phase modulation of metasurfaces for the output layer of sensors processes the diffractive field. The optical intensities in the predefined detection zones are extracted from the output image, and the predicted results are decoded to generate the control signals in the games. Then the new frame image of the video game stimulates the new process procedure, and the updated results control the game until the end.

2.2 Playing Tic-Tac-Toe

In our first implementation, we perform the polarization-multiplexed decision-making and control for Tic-Tac-Toe. It is a two-person game played on a board, and the two players take turns while each player claims a single one of the squares with the piece (traditionally X and O). The first player to make three pieces in a row vertically, horizontally, or diagonally wins the game. If all squares are filled, and neither player

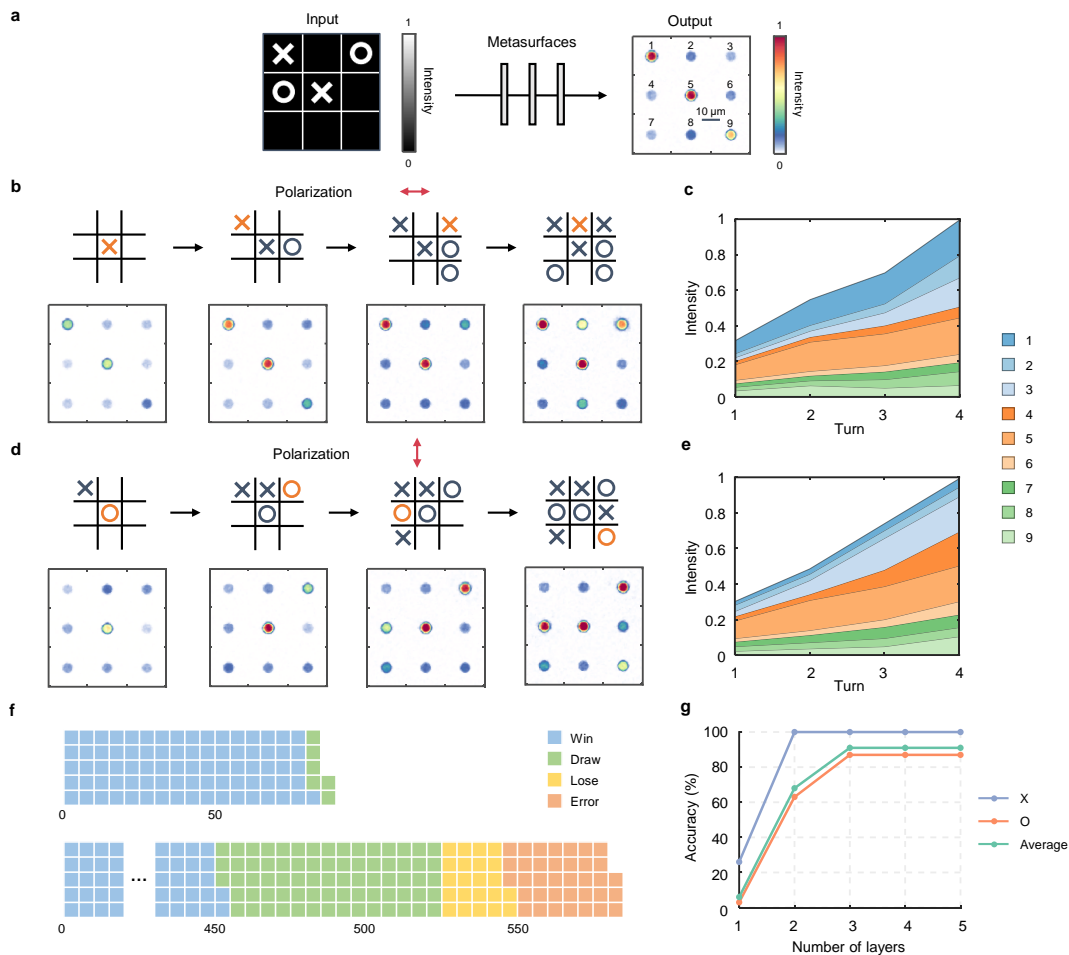


Fig. 3 **Playing Tic-Tac-Toe.** **a** The schematic illustration of the diffractive network composed of an input layer, hidden layers of cascaded three-layer metasurfaces, and an output layer for playing Tic-Tac-Toe. **b–e** The sequential control of the polarization-multiplexed diffractive network in performing gameplay tasks for the X and O pieces, respectively. **f** The accuracy rate of playing Tic-Tac-Toe. There is a collection of 87 games utilized for predicting the X piece, obtaining 81 wins and 6 draws in these games. In the rest of the 583 games, the O piece obtains 452 wins, 73 draws, and 22 losses. When previous moves have occupied the predicted position at a turn, such a case is counted as a playing error and occurs 36 times. **g** Dependence of the prediction accuracy on the number of hidden layers.

has three pieces in a row, the game is declared a draw. There are 255,168 possible ways to play this game, and we use the proposed network architecture to capture the effective policies to allow optimal playing performance.

For playing this game, the network composed of three-layer transmissive metasurfaces is designed by the training algorithm above; see Supplementary Fig. 4 for phase profiles. The input images carrying the information of the current states are encoded into the amplitude of the input field to the network, and the network is trained to

map incident energy into nine squares corresponding to the 3×3 board (marked by the number 1–9) where the receiving energy distribution at each region reveals the current state and predict the probability of the next move of the player, as shown in Fig. 3a. Since the observed state and the action are both discrete in this game, the Tic-Tac-Toe can be considered as a demonstration of our method for a collection of tasks with discrete state and action spaces.

Note that the first (X) and second (O) players would have different control policies, that is, the X piece seeks a win, and O tries to draw in

the ideal case. Thus, the polarization-multiplexed metasurface-based diffractive network is jointly optimized using our training framework. Specifically, the X piece is assigned to the x linear input and output polarization combination, and O is assigned to the y linear input and output polarization combination. After training, the X piece moves of every turn are illustrated in Fig. 3b under the x-polarization combination. In the first turn, three possible positions, 1, 5, and 9, are predicted as depicted on the board, but the starting position of 5 is finally chosen due to the maximum energy intensity amongst these positions. After the O piece responds to X, the input image changes, and in the second turn, the intensity distributions of the output also change so that the predicted move of X is determined at the position of 1 by extracting the maximum signal amongst the unoccupied positions. It is also noted that the output intensity will focus not only on the predicted position but also on the current states with positions occupied. Following this prediction and control procedure, the first player wins in the fourth turn in Fig. 3b. In the same principle, the O piece moves are predicted and controlled under y polarization, shown in Fig. 3d. It can be observed that the O piece responds to a corner opening with a center piece and selects moves next to the X to avoid the opponent having three pieces in a row. In such a way, the O piece avoids the win of X. This optimal policy is successfully used in the proposed network, and a draw game result is shown in Fig. 3d, while the O piece may gain a win if X makes a weak play in some particular cases.

While, in general, a human player aims to win the game, Tic-Tac-Toe will end in a draw if both players play their best because it is a zero-sum game. To evaluate the accuracy and effectiveness of our proposed network in playing Tic-Tac-Toe, we use the sum of the win and draw rate as the accuracy rate. After the self-play training per game rules, we numerically test the design of the diffractive network with all possible states, as shown in Fig. 3f. The policy we trained is optimal and will only choose the best moves, so only 670 states will appear. Among them, the accuracy rate of X is 100%, the accuracy rate of O is 90.05%, and the average rate is 91.34%. The accuracy of the network in predicting the O piece shows a slight degradation relative to that of X due to the factors such as more complex policy and more states

of O. On the other hand, we evaluate the dependence of the prediction accuracy on the numbers of hidden layers in Fig. 3g. The increasing number of layers accompanied by increasing neurons and interconnections in the diffractive network improves the performance in Tic-Tac-Toe for both playing the X and O pieces under different polarizations. However, the accuracy does not show a noticeable change when the layer number continues to increase from 3, which may be caused by the reason that the diffractive network is unsuitable for predicting states with only local differences or high similarity[52]; see Supplementary Note 6 for detailed derivation.

2.3 Playing Super Mario Bros.

In our second implementation, the testbed platform game used for the diffractive network is the world 1-1 of the original Super Mario Bros. Different from the Tic-Tac-Toe on a square-divided board, Super Mario Bros. is a video game with continuous high-dimensional state inputs. The gameplay consists of moving the player-controlled character, Mario, through two-dimensional levels to get to the level's end, traversing it from left to right, avoiding obstacles and enemies, and interacting with game objects. In the game, the player controls Mario to take discrete actions run, jump, and crouch. Under these considerations, this game can be an example of continuous state space and discrete action space for testing the proposed network.

Fig. 4a illustrates the metasurface-based diffractive neural network for playing Super Mario Bros. The network consists of an input layer carrying the optical field encoded from each video game frame, hidden layers composed of cascaded five-layer transmissive metasurfaces trained by the same algorithm, and the output layer mapping the intensity distribution into preset regions; see Supplementary Fig. 5 for phase profiles. It is clear that the input images from the game scene consisting of moving backgrounds and different objects are more complex relative to the Tic-Tac-Toe board with a regular pattern. In addition, the game images are similar between adjacent ones and constantly changing due to the gameplay on a side-scrolling platform, which challenges the diffractive network in processing highly similar input states for choosing optimal actions.

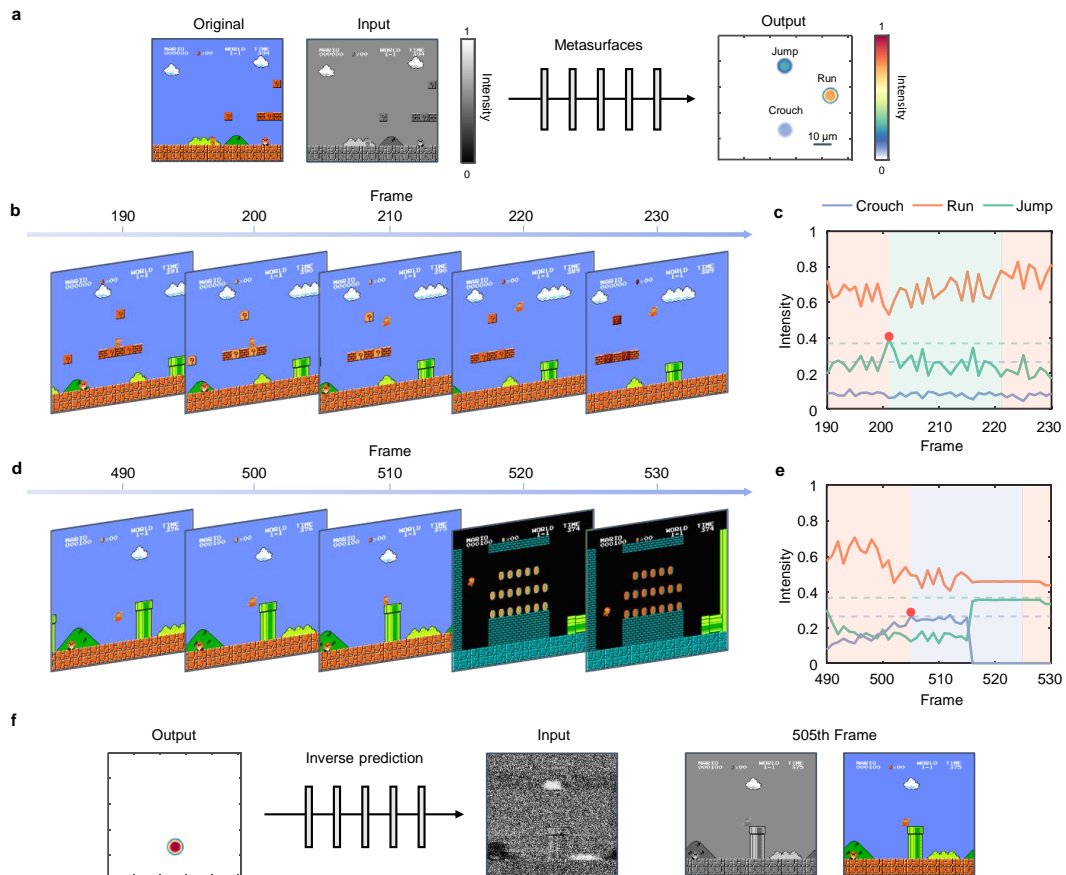


Fig. 4 Playing Super Mario Bros. **a** The layout of the designed network for playing Super Mario Bros. **b–e** Snapshots of Mario’s jumping and crouching actions by comparing the corresponding output intensity with respect to their respective threshold. When the predicted action is to jump as the output intensity for jumping exceeds the preset threshold at the 203rd frame in **c**, Mario is controlled to perform this action, shown in **b**. A similar series of prediction and control for another crouching action can also be observed in **d**, **e**. **f** The inverse prediction result. Considering the predicted crouching at the current state is crucial to update Mario’s action, we use the maximal output intensity for crouching as the input ignoring the simultaneous output for other actions.

After training with the control policy, the network makes decisions for Mario’s optimal action and achieves accurate control to reach the end of the level until taking down the flag raised above the castle, as shown in Supplementary Video 1. Specifically, at any given state, the most optimal action that Mario chooses to take is predicted by referring to the preset threshold measured in the training process. In the examples of Fig. 4b–e, we take some snapshots from Supplementary Video 1 to analyze the decision-making and control of Mario’s actions in complex, time-varying configurations. Since our network’s goal is to finish the level as fast as possible successfully, Mario should keep the run action until the end while he chooses

to jump or crouch to overcome the challenges at certain states. Thus, the output intensity for running action keeps high throughout the game, while the intensity for jump and crouch shows fluctuations with respect to their thresholds, verified by Fig. 4c,e. Although this significant intensity triggers the prediction only at a particular frame, this control signal is intentionally set to last for 20 frames to guarantee Mario’s finishing the entire action. It is worth noting that the intensity-frame curve remains relatively stable during the 516th to 530th frame, which can be understood with the static and high-contrast background images after Mario goes into the pipe, as shown in Fig. 4d.

To gain an insight into how the diffractive neural network makes decisions, we investigate the network's perception capability, employing inverse prediction in Fig. 4f. We demonstrate what the network has learned from the high-dimensional sensory input to perform the crouching action corresponding to the 505th frame image. We use the error back-propagation algorithm in the same diffractive network to inversely predict the input image at this moment; see Supplementary Note 4 for detailed derivation. The inversely predicted image matches the original input image of the 505th frame, especially the background, such as clouds and grasses. When humans play the game, they may ignore these backgrounds and only focus on the critical parts, such as Mario, enemies, and pipes. The inverse prediction of the whole scene highlights the capability of the network to extract global features instead the local ones, further verifying the perception capability of the network in capturing the global features to make decisions.

2.4 Playing Car Racing

Finally, we demonstrate the proposed network capability in the car racing game, which requires perceiving the game environment using continuous high-dimensional inputs and making decisions to control the car's taking continuous steering actions. The game's control policy is trained based on the rules of keeping the car within the racetrack by controlling its rotation, and the car is set to increase the speed once the game starts. The diffractive network architecture is designed in Fig. 5 and in a similar form to previous examples. The input energy of the optical field is redistributed through four metasurface diffractive layers into the two designated regions on the left and right of the output layer; see Supplementary Fig. 6 for phase profiles. The difference value between the intensities at the current state controls the steering direction and angle of the car shown in Fig. 5b. In addition, just as in the steering dead zone in actual vehicles, a slight difference value would not lead to steering action to avoid disturbance.

The successful network implementation in the racing game is illustrated in Supplementary Video 2 where the car is controlled in the center of the racetrack almost within the whole lap. For the two basic actions of the left and right turn, some exemplary snapshots are provided in Fig. 5c-j.

Specifically, the negative difference values in Fig. 5d predict the turning left of the car wheel, while the larger absolute values indicate sharper turns. It is also observed that sometimes the difference values approach zero, and a rotation angle of 0 is predicted to keep the car racing in the direction of the current state. Due to the larger turning angle of the lane, the different intensities for turning left exhibit a more drastic change. It is also intriguing that although the car steering in the left turn shows unsmooth disconnected to some extent so that it does not appear in the middle of the racetrack at certain states, the controlled action that is updated in the following state leads to successful gameplay. This real-time feedback and updating feature shows the great potential of the architecture in challenging auto-driving almost at the speed of light, such as dealing with sudden obstacles.

To validate the interference immunity of the training approach and the proposed network, we introduce two crucial randomization interference mechanisms to the frame image of the game and then test the network performance in online controlling of car racing. With the same network previously trained, Gaussian blur and Gaussian noise are respectively added to the frames, and the control results are shown in Fig. 5e,f and Fig. 5i,j, respectively. Note that the exerted interferences are the maximal value before they reach the limit of affecting the car racing control of the game. Although the introduction of interference, including blurring and noises, causes the quality decline of the input image, the car racing can obtain accurate and effective control to successfully complete the game, verified by Supplementary Videos 3 and 4. Compared with ordinary control in Fig. 5d,h, the output intensity curves in Fig. 5f,j show consistent trends to control the turning left or right actions. However, the curves are less smooth with more amplitude fluctuations implying an unsmooth control in steering angle. The successful control in the cases with the randomization interference reveals the great perception from the game environment, especially the full access to the global features.

3 Discussion

We have demonstrated metasurface-based diffractive neural networks for decision-making and

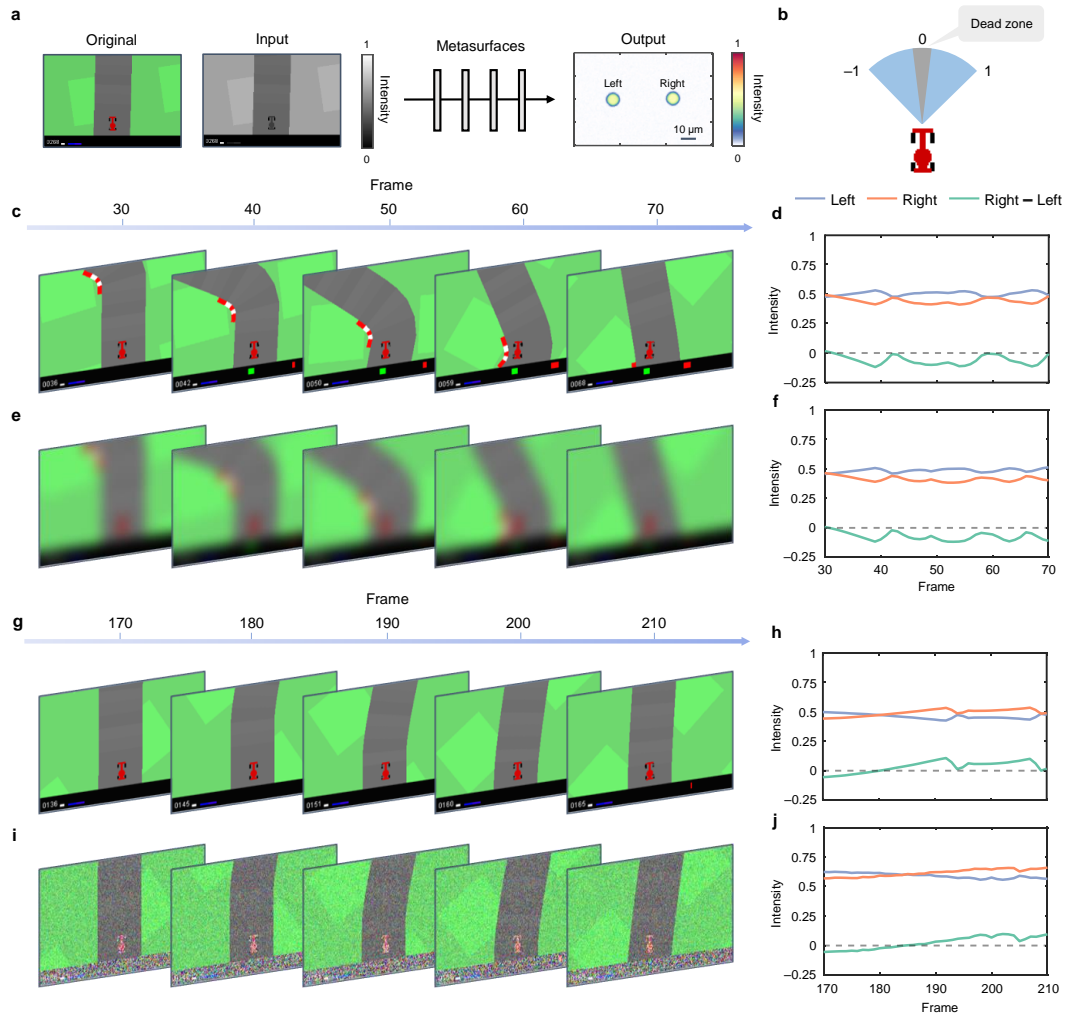


Fig. 5 Playing Car Racing. **a** The layout of the designed network for playing car racing. **b** The control of the steering direction and angle of the car with respect to the difference value between the intensities at the current state, normalized between -1 and 1 . **c–j** Snapshots of controlling the car steering. When the car is faced a left-turn lane in **c**, the output intensity on the left keeps the value greater than or equal to the right intensity, allowing continuous control in updating the rotation angle of the left-turn action. A similar control process can also be carried out for the right-turn lane in **g**, **h**. In addition, the interference immunity of the network is validated by introducing the Gaussian blur **e**, **f** and Gaussian noise **i**, **j** to the game images, respectively.

control. The optimal control policy enables this technique through a harmonious combination of deep reinforcement learning and the diffractive network architecture. Based solely on reinforcement learning from self-play, the control policy of the training algorithm is flexible, as demonstrated by successfully learning to play the three types of classic games. It is worth noting that Tic-Tac-Toe does not achieve perfect results despite the definite rules and optimal control policy, just like Super Mario Bros. and Car Racing. There

are several possible reasons for this result: Playing Tic-Tac-Toe needs to strategically handle different states and a more significant number of output signals. The gameplay of Tic-Tac-Toe requires correct predictions at each state, while the other two games show better error tolerance, and accidental mistakes do not necessarily affect the results. In addition, using the difference and threshold as a mechanism to trigger actions also improves the network's performance in the other two games to some extent. Since the diffractive network is not

good at extracting local features, the differences in intensity distributions between the adjacent input board images are challenging to detect for Tic-Tac-Toe.

By testing our proposed diffractive network on the challenging domain of classic games, we demonstrate that the network can achieve a level comparable to human players, which is also the first time on an optical platform. This work bridges the gap between the neuromorphic metasurface and the digital neural network aiming to achieve human-level AI. The most important aspect is that the decision-making and control process is entirely implemented in an optical circuit at the speed of light by imitating human competency. An all-optical system could be envisioned if an optical game platform is available and the control signal triggered by electric sensors is replaced by optical feedback signals such as optical intensity. Since the test games are on an electric computer platform, the electric sensors are used in the system to complete the optical-to-electrical conversion.

Despite the exciting results of playing games, the metasurface diffractive neural network currently has limitations for handling more complex tasks. For the sake of the computational requirements of optical forward propagation, we deploy a two-phase training architecture to obtain the policy model before iterating the diffractive network instead of end-to-end learning in this work. Combining the two steps may reduce errors and make it easier to use. In addition, the inference and control capability of diffractive networks could also be improved by introducing methods such as nonlinear optical effects[53–56], residual structures[57], and Fourier space[33] in the future, leading to a variety of new applications. While preliminary, this research suggests that the metasurface diffractive neural network has great potential for processing complex visual inputs and tasks. It could provide a promising avenue for an integrable optical system for decision-making and control, which would be a fruitful area for next-generation AI.

4 Methods

4.1 Training of diffractive neural network

We use the open-source machine learning framework Pytorch to build the training algorithm. The training process is implemented using Python (v3.9.13), Gym (v0.21.0) environment, and Pytorch (v1.11.0) framework on a desktop computer with AMD Ryzen 9 5950X CPU, Nvidia GeForce RTX 3080 Ti GPU, and 64 GB RAM.

We train each diffractive network individually. The neuron numbers per layer of diffractive network are 150×150 , 256×240 , and 300×200 for Tic-Tac-Toe, Super Mario Bros., and Car Racing. In the iterative process of a diffractive network, the learning rate is 0.01, the number of training epochs is 1000, and constrain the phase-modulation range to $0-2\pi$ for training. In addition, due to the unbalanced number of occurrences of output action, such as jump and crouch are far rarer than run in Super Mario Bros., we balance these actions by altering the weight that each training example carries when computing the loss. Training of the network takes about a few minutes to tens of minutes. After training, the network’s performance is verified by interaction with the game environment.

4.2 Modeling of control policy

We train different control policies on each game using the same network architecture, learning algorithms, and hyperparameter settings. That shows our approach is robust enough to work on various games while incorporating only minimal prior knowledge. PPO uses two neural network architectures to design and optimize the policy: the critic network and the actor-network. Both networks are adapted during training, but only the actor-network is deployed as the control policy. Specifically, for the actor-network, The input to the CNN consists of a 128×128 grayscale image produced by the preprocessing. The first hidden layer convolves 32 filters of 8×8 with stride 4 with the input image. The second hidden layer convolves 64 filters of 4×4 with stride 2. This is followed by a third convolutional layer convolving 64 filters of 3×3 with stride 1. The final hidden layer is fully-connected with 512 latents. Each hidden layer is followed by a rectified linear

unit (ReLU). The output layer is a fully-connected linear layer with a single output for each valid action. The critic network is also a CNN which is about the same as the actor-network, except the output represents the discounted expected future reward for various actions. The reward functions are detailed in Supplementary Note 3. The learning rate is 0.001, and the discount is 0.99. In addition, because consecutive frames do not vary much, we can skip 4 intermediate frames without losing much information to accelerate training. Train of the control policy takes about an hour to a dozen hours. After the training, we save each game frame and the corresponding action for diffraction network training.

4.3 Design of metasurface

The hidden layers are composed of cascaded multi-layer metasurfaces constructed through a honeycomb lattice with hexagonal units. Each diffractive metasurface comprises carefully arranged rectangular silicon nanopillars on a quartz substrate. Each meta-unit can be represented as a neuron with a complex-valued transmission coefficient. The hidden layers are intended to decide the best move and image of the calculated result at the output layer.

Specifically, the center-to-center spacing of adjacent nanopillars is 300 nm, the length of a side of the hexagon L is 173.2 nm, the height H is 300 nm, and the layer-to-layer distance is 50 μm . By adjusting these nanopillars' geometry parameters (D_x, D_y), we can modify the phase above the elements in response to a plane wave. With the knowledge of the phase in terms of the geometry parameters, it is possible to create a metasurface with an arbitrary phase profile by placing the meta-units at the necessary positions. We used the finite difference time domain (FDTD) simulation tool to model a unit cell. Then we swept the geometry parameters of the nanopillars and obtained the phase and transmission.

Data availability

All data are available in the main text or the supplementary materials.

Code availability

The code used for the analyses will be made available upon e-mail request to the corresponding authors.

References

- [1] Krizhevsky, A., Sutskever, I. & Hinton, G. E. Imagenet classification with deep convolutional neural networks. *Commun. ACM* **60** (6), 84–90 (2017).
- [2] Russakovsky, O. *et al.* Imagenet large scale visual recognition challenge. *International Journal of Computer Vision* **115** (3), 211–252 (2015).
- [3] Chen, Q. *et al.* Enhanced LSTM for natural language inference, In *Proceedings of the 55th Annual Meeting of the Association for Computational Linguistics*, 1657–1668 (2017).
- [4] Devlin, J., Chang, M.-W., Lee, K. & Toutanova, K. BERT: Pre-training of deep bidirectional transformers for language understanding, In *2019 Annual Conference of the North American Chapter of the Association for Computational Linguistics*, 4171–4186 (2019).
- [5] Grover, A. & Leskovec, J. Node2vec: Scalable feature learning for networks, In *Proceedings of the 22nd ACM SIGKDD International Conference on Knowledge Discovery and Data Mining*, 855–864 (2016).
- [6] Ma, W. *et al.* Deep learning for the design of photonic structures. *Nature Photonics* **15** (2), 77–90 (2021).
- [7] Jiang, J. & Fan, J. A. Simulator-based training of generative neural networks for the inverse design of metasurfaces. *Nanophotonics* **9** (5), 1059–1069 (2020).
- [8] Khatib, O., Ren, S., Malof, J. & Padilla, W. J. Learning the physics of all-dielectric metamaterials with deep lorentz neural networks. *Advanced Optical Materials* **10** (13), 2200097 (2022).

- [9] Gao, L., Li, X., Liu, D., Wang, L. & Yu, Z. A bidirectional deep neural network for accurate silicon color design. *Advanced Materials* **31** (51), 1905467 (2019).
- [10] Huang, L., Xu, L. & Miroschnichenko, A. E. *Deep learning enabled nanophotonics*. in *Advances and Applications in Deep Learning* (ed. Aceves-Fernandez, M. A.) Ch. 4 (IntechOpen, London, 2020).
- [11] Xu, L. *et al.* Enhanced light-matter interactions in dielectric nanostructures via machine-learning approach. *Advanced Photonics* **2** (2), 026003 (2020).
- [12] Wiecha, P. R. & Muskens, O. L. Deep learning meets nanophotonics: A generalized accurate predictor for near fields and far fields of arbitrary 3d nanostructures. *Nano Letters* **20** (1), 329–338 (2020).
- [13] Dai, P. *et al.* Accurate inverse design of Fabry-Perot-cavity-based color filters far beyond sRGB via a bidirectional artificial neural network. *Photon. Res.* **9** (5), B236–B246 (2021).
- [14] Dai, P. *et al.* Inverse design of structural color: finding multiple solutions via conditional generative adversarial networks. *Nanophotonics* **11** (13), 3057–3069 (2022).
- [15] Khatib, O., Ren, S., Malof, J. & Padilla, W. J. Deep learning the electromagnetic properties of metamaterials—a comprehensive review. *Advanced Functional Materials* **31** (31), 2101748 (2021).
- [16] Nadell, C. C., Huang, B., Malof, J. M. & Padilla, W. J. Deep learning for accelerated all-dielectric metasurface design. *Opt. Express* **27** (20), 27523–27535 (2019).
- [17] Li, T. *et al.* Photonic-dispersion neural networks for inverse scattering problems. *Light: Science & Applications* **10** (1), 154 (2021).
- [18] Deng, Y., Ren, S., Fan, K., Malof, J. M. & Padilla, W. J. Neural-adjoint method for the inverse design of all-dielectric metasurfaces. *Opt. Express* **29** (5), 7526–7534 (2021).
- [19] Shen, Y. *et al.* Deep learning with coherent nanophotonic circuits. *Nature Photonics* **11** (7), 441–446 (2017).
- [20] Feldmann, J., Youngblood, N., Wright, C. D., Bhaskaran, H. & Pernice, W. H. P. All-optical spiking neurosynaptic networks with self-learning capabilities. *Nature* **569** (7755), 208–214 (2019).
- [21] Hamerly, R., Bernstein, L., Sludds, A., Soljačić, M. & Englund, D. Large-scale optical neural networks based on photoelectric multiplication. *Phys. Rev. X* **9**, 021032 (2019).
- [22] Zhang, H. *et al.* An optical neural chip for implementing complex-valued neural network. *Nature Communications* **12** (1), 457 (2021).
- [23] Liu, J. *et al.* Research progress in optical neural networks: theory, applications and developments. *Photonix* **2** (1), 5 (2021).
- [24] Zhou, H. *et al.* Photonic matrix multiplication lights up photonic accelerator and beyond. *Light: Science & Applications* **11** (1), 30 (2022).
- [25] Lin, X. *et al.* All-optical machine learning using diffractive deep neural networks. *Science* **361** (6406), 1004–1008 (2018).
- [26] Wu, Z., Zhou, M., Khoram, E., Liu, B. & Yu, Z. Neuromorphic metasurface. *Photon. Res.* **8** (1), 46–50 (2020).
- [27] Chen, H. *et al.* Diffractive deep neural networks at visible wavelengths. *Engineering* **7** (10), 1483–1491 (2021).
- [28] Qian, C. *et al.* Dynamic recognition and mirage using neuro-metamaterials. *Nature Communications* **13** (1), 2694 (2022).
- [29] Zhou, T. *et al.* Large-scale neuromorphic optoelectronic computing with a reconfigurable diffractive processing unit. *Nature Photonics* **15** (5), 367–373 (2021).

- [30] Liu, C. *et al.* A programmable diffractive deep neural network based on a digital-coding metasurface array. *Nature Electronics* **5** (2), 113–122 (2022).
- [31] Zheng, H. *et al.* Meta-optic accelerators for object classifiers. *Science Advances* **8** (30), eabo6410 (2022).
- [32] Xu, Z., Yuan, X., Zhou, T. & Fang, L. A multichannel optical computing architecture for advanced machine vision. *Light: Science & Applications* **11** (1), 255 (2022).
- [33] Yan, T. *et al.* Fourier-space diffractive deep neural network. *Phys. Rev. Lett.* **123**, 023901 (2019).
- [34] Qian, C. *et al.* Performing optical logic operations by a diffractive neural network. *Light: Science & Applications* **9** (1), 59 (2020).
- [35] Dorrah, A. H. & Capasso, F. Tunable structured light with flat optics. *Science* **376** (6591), eabi6860 (2022).
- [36] Huang, L. *et al.* Three-dimensional optical holography using a plasmonic metasurface. *Nature Communications* **4** (1), 2808 (2013).
- [37] Zheng, G. *et al.* Metasurface holograms reaching 80% efficiency. *Nature Nanotechnology* **10** (4), 308–312 (2015).
- [38] Jin, L. *et al.* Noninterleaved metasurface for (2^6-1) spin- and wavelength-encoded holograms. *Nano Letters* **18** (12), 8016–8024 (2018).
- [39] Ren, H. & Maier, S. A. Nanophotonic materials for twisted-light manipulation. *Advanced Materials*, 2106692 (2021).
- [40] Li, L. *et al.* Machine-learning reprogrammable metasurface imager. *Nature Communications* **10** (1), 1082 (2019).
- [41] Deng, L. *et al.* Malus-metasurface-assisted polarization multiplexing. *Light: Science & Applications* **9** (1), 101 (2020).
- [42] Liu, T., Han, Z., Duan, J. & Xiao, S. Phase-change metasurfaces for dynamic image display and information encryption. *Phys. Rev. Applied* **18**, 044078 (2022).
- [43] Padilla, W. J. & Averitt, R. D. Imaging with metamaterials. *Nature Reviews Physics* **4** (2), 85–100 (2022).
- [44] Luo, X. *et al.* Metasurface-enabled on-chip multiplexed diffractive neural networks in the visible. *Light: Science & Applications* **11** (1), 158 (2022).
- [45] Schulman, J., Wolski, F., Dhariwal, P., Radford, A. & Klimov, O. Proximal policy optimization algorithms. Preprint at <https://arxiv.org/abs/1707.06347> (2017).
- [46] Kingma, D. P. & Ba, J. Adam: A method for stochastic optimization. In *3rd International Conference on Learning Representations* (2015).
- [47] Artar, A., Yanik, A. A. & Altug, H. Multispectral plasmon induced transparency in coupled meta-atoms. *Nano letters* **11** (4), 1685–1689 (2011).
- [48] Zhou, Y. *et al.* Multifunctional metaoptics based on bilayer metasurfaces. *Light: Science & Applications* **8** (1), 80 (2019).
- [49] Goi, E. *et al.* Nanoprinted high-neuron-density optical linear perceptrons performing near-infrared inference on a cmos chip. *Light: Science & Applications* **10** (1), 40 (2021).
- [50] Goi, E., Schoenhardt, S. & Gu, M. Direct retrieval of zernike-based pupil functions using integrated diffractive deep neural networks. *Nature Communications* **13** (1), 7531 (2022).
- [51] Wang, Z., Qian, C., Fan, Z. & Chen, H. Arbitrary polarization readout with dual-channel neuro-metasurfaces. *Advanced Science*, 2204699 (2021).
- [52] Zheng, S., Xu, S. & Fan, D. Orthogonality of diffractive deep neural network. *Opt. Lett.* **47** (7), 1798–1801 (2022).

- [53] Schlickriede, C. *et al.* Nonlinear imaging with all-dielectric metasurfaces. *Nano Letters* **20** (6), 4370–4376 (2020).
- [54] Xiao, Y., Qian, H. & Liu, Z. Nonlinear metasurface based on giant optical kerr response of gold quantum wells. *ACS Photonics* **5** (5), 1654–1659 (2018).
- [55] Akie, M., Fujisawa, T., Sato, T., Arai, M. & Saitoh, K. GeSn/SiGeSn multiple-quantum-well electroabsorption modulator with taper coupler for mid-infrared Ge-on-Si platform. *IEEE Journal of Selected Topics in Quantum Electronics* **24** (6), 1–8 (2018).
- [56] Zuo, Y. *et al.* All-optical neural network with nonlinear activation functions. *Optica* **6** (9), 1132–1137 (2019).
- [57] Dou, H. *et al.* Residual D2NN: training diffractive deep neural networks via learnable light shortcuts. *Opt. Lett.* **45** (10), 2688–2691 (2020).

Acknowledgments

This work was supported by the National Natural Science Foundation of China (Grant Nos. 12064025, 11947065, and 12264028); the Key Research and Development Program of Jiangxi Province (Grant No. 20192BBE50058); the Natural Science Foundation of Jiangxi Province (Grant Nos. 20212ACB202006 and 20202BAB211007); the Major Discipline Academic and Technical Leaders Training Program of Jiangxi Province (Grant No. 20204BCJ22012); the Shanghai Pujiang Program (Grant No. 22PJ1402900); the Australian Research Council Discovery Project (Grant No. DP200101353); the Interdisciplinary Innovation Fund of Nanchang University (Grant No. 2019-9166-27060003).

Author Contributions

J.Q. and S.X. conceived the idea. J.Q. performed the theoretical calculation and numerical simulations. J.Q., T.Y., L.H., and A.M. helped with the theoretical interpretation. T.Y., L.H., and S.X. supervised the project. All authors discussed the results and prepared the manuscript.

Competing Interests

The authors declare no competing interests.